

# Enhancing Post-Disaster Mapping Assessment: Agent-Based Simulation Modeling Integrating Ground Vehicles and Drones (Case Study: Mount Merapi's Volcanic Eruption)

Rahmad Inca Liperda <sup>1\*</sup>, Ravi Prananda Rinaldy <sup>1</sup>, Anak Agung Ngurah Perwira Redi <sup>2</sup>, Anna Maria Sri Asih <sup>3</sup>, Bertha Maya Sopha <sup>3</sup>

<sup>1</sup> Pertamina University, Kota Jakarta Selatan, DKI Jakarta 12220, Indonesia

<sup>2</sup> Faculty of Engineering and Technology, Sampoerna University, Jakarta 12780, Indonesia

<sup>3</sup> Department of Mechanical and Industrial Engineering, Universitas Gadjah Mada (UGM), Yogyakarta, Indonesia

Email : inca.liferda@universitaspertamina.ac.id

\* Corresponding author

## ARTICLE INFO

### Article history

Received : 11-11-2023

Revised : 13-11-2023

Accepted : 24-11-2023

### Keywords

Agent-based Simulation;  
Post-Disaster Mapping Assessment;  
Eruption;

## ABSTRACT

*This research presents an agent-based simulation model for post-disaster location mapping, considering land vehicles and drones along with access road availability and depot locations. The study examines the impact of bridge facility damage on depot selection and time indicators. Results reveal that damage to bridge facilities affects depots differently based on their location, leading to increased total processing and completion times due to interactions between land vehicles and bridges. Depot 7 emerges as the optimal location for undamaged and KRB II and III damage scenarios based on total processing time. Depot 3 performs best for KRB III damage, while Depot 8 exhibits the shortest completion time across all scenarios. These findings emphasize the importance of selecting depots with resilient road access and alternative routes, improving post-disaster logistics efficiency.*

## 1. INTRODUCTION

A disaster is an event that can cause extensive disruption to society or communities [1]. Such disruptions often encompass human casualties, material and economic losses, as well as environmental and infrastructural damage. The unpredictable and sudden nature of disasters underscores the need for an immediate, efficient, and coordinated response from diverse sectors. This collective effort is crucial for effectively managing and mitigating the consequences of disasters, ensuring a timely recovery and minimizing their long-term impacts.

Indonesia is recognized as one of the countries highly vulnerable to natural hazards, ranking 38th globally in terms of disaster risk [2]. Its geographical location within the ring of fire renders Indonesia particularly susceptible to earthquakes and volcanic eruptions [3]. With a staggering count of 147 volcanoes, Indonesia stands out as one of the nations with the highest volcano abundance worldwide [4]. Among these volcanoes, Mount Merapi holds significant prominence as it is listed among the 16 Decade Volcanoes by the International Association of Volcanology and Chemistry of the Earth's Interior (IAVCEI), signifying its status as an active and highly risky volcano [5]. Mount Merapi exhibits a notably short eruption cycle of 2-7 years and poses various hazards to human lives, infrastructure, and essential resources such as agriculture, livestock, shelters, and transportation routes [6]. In 2010, Mount Merapi unleashed a particularly explosive eruption classified as a Volcanic Explosivity Index (VEI) of 4, resulting in 347 fatalities and displacing 410,388 individuals [6] [7].

Disaster management encompasses a planning and administrative process aimed at mitigating the burden and consequences of disasters. It consists of four distinct stages: mitigation, preparedness, response, and recovery [8]. A widely adopted approach during the response and recovery stages is the Post-Disaster Needs Assessment (PDNA), internationally endorsed by the European Union (EU), World Bank (WB), and United Nations Development Group (UNDG) in 2008. PDNA serves as a comprehensive framework for assessing the impact of a disaster, focusing on four sectors: social, productive, infrastructure, and cross-cutting. These sectors are discussed within the PDNA guidelines,

which cover aspects ranging from evaluating post-disaster damages and losses to formulating recovery strategies and plans [9].

The initial step of the PDNA involves the collection of data pertaining to the post-disaster conditions [9]. This data collection activity falls within the response phase of disaster management and holds significant importance, as it provides essential information on the extent of impacts, victim locations, casualty numbers, and logistical requirements for efficient post-disaster operations. The timeliness and responsiveness of data collection concerning the post-disaster situation must be prioritized, as these factors serve as benchmarks for assessing the logistical capabilities required to save lives and expedite infrastructure repairs [10]. A viable approach to gathering data on the physical impacts of the disaster is through the mapping of affected areas. This process enables the accurate spatial visualization of the disaster-affected regions, serving as a foundation for information used in disaster management operations [11].

An obstacle commonly encountered during post-disaster logistics operations is the impairment of road infrastructure, resulting in inaccessible roadways [12]. This hampers the thorough utilization of land vehicles for mapping affected areas. To address this challenge, the implementation of Unmanned Aerial Vehicles (UAVs), commonly known as drones, offers a viable solution. Drones possess the advantages of flexibility, cost-effectiveness, and speed, making them suitable for efficiently capturing photo and video documentation to map disaster-affected locations [13]. However, the use of drones for mapping purposes has limitations, such as their restricted range and limited operational duration. Overcoming these limitations can be achieved by combining land vehicles and drones in the mapping process. While land vehicles face range limitations based on road accessibility, they have longer operational durations compared to drones. Therefore, employing a combination of land vehicles and drones compensates for each other's shortcomings, effectively addressing road access issues with drones and resolving operational time and range challenges with land vehicles [10].

In the scenario of mapping post-disaster locations through a combination of land vehicles and drones, the process unfolds as follows. Initially, each land vehicle carries a single drone unit from the depot to a predetermined stopover point. Upon arrival at the stopover point, the land vehicle sets up the drone, which then commences mapping various pre-identified points. In the event of the drone's battery reaching a low charge during the mapping process, it promptly returns to the stopover point for a battery replacement. Once the battery is replaced, the drone resumes mapping any remaining unmapped points. After all the designated mapping points have been covered, the drone returns to the stopover point for dismantling, and the land vehicles transport it back to the depot. Subsequently, the obtained mapping results of the disaster-affected locations can be promptly reported and processed for the purpose of Post-Disaster Needs Assessment (PDNA). A visual representation of the scheme depicting the combination of land vehicle and drone routes can be observed in Figure 1, where red dots represent depots, green dots signify stopover points, blue dots indicate mapping points, blue arrows represent land vehicle routes, and red arrows depict drone routes.

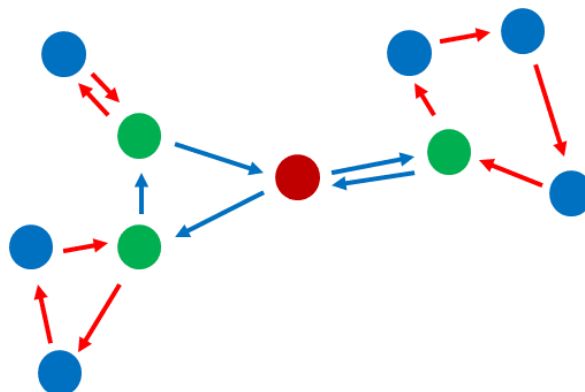


Fig. 1 The approach of mapping post-disaster locations using a combined route of ground vehicles and drones has been proposed [10].

The process of post-disaster mapping assessment is subject to various uncertainties, both from the perspective of the mapping actor and the environmental conditions in which the mapping takes place. Uncertainties originating from the mapping actor's side may involve factors such as vehicle speed, preparation time for mapping activities, or operational aspects like drone setup and disassembly duration. Conversely, uncertainties arising from the environmental side pertain to variables such as weather conditions and the accessibility of existing infrastructure. In the context of post-disaster location mapping, the accessibility of infrastructure, particularly land vehicle lanes, holds great significance. The presence of accessible land vehicle routes is essential for smooth mobilization. However, in the aftermath of an eruption, certain infrastructure elements like bridges can be profoundly affected. The movement of cold lava flows over rivers or streams can erode bridge foundations, leading to their collapse [14]. Consequently, mapping actors who initially planned to utilize a bridge must reassess alternative routes to reach their designated mapping points.

Mount Merapi is characterized by multiple regions that are susceptible to disasters, known as Kawasan Rawan Bencana (KRB). The KRB is further categorized into three distinct areas [15]:

- 1) *KRB III refers to regions frequently impacted by volcanic projectiles, lava streams, hazardous gases, pyroclastic rock avalanches, or pyroclastic flows during volcanic eruptions or related activities.*
- 2) *KRB II designates areas with the potential to experience volcanic debris avalanches, lava flows, noxious gases, pyroclastic rock avalanches, intense ash precipitation, or pyroclastic flows when volcanic eruptions or related activities occur.*
- 3) *KRB I encompasses areas at risk of being affected by lava flows or flooding.*

The KRB (Kawasan Rawan Bencana) map of Mount Merapi serves as a valuable tool for assessing the vulnerability of an area to the volcano's eruption. Higher KRB numbers indicate a greater risk of impact in the event of a Mount Merapi eruption, necessitating focused attention on these areas. However, challenges such as operational uncertainties and road accessibility issues can impede the post-disaster mapping assessment process, including in the case of Mount Merapi's eruption. Therefore, it is crucial to consider and comprehend these factors to ensure the efficiency of post-disaster site mapping. Scenario development in research offers a method to gain a comprehensive understanding of the implications of problems or decisions within the entire system [16]. For instance, one scenario may involve analyzing the availability of road access for land vehicles based on the distribution within the KRB. Another scenario could revolve around the decision-making process for selecting an appropriate depot location responsible for mapping post-disaster locations. However, conducting research by directly developing scenarios within real systems is impractical due to the extensive time and resources required. An alternative solution is to employ agent-based simulation models for scenario development.

Agent-based simulation is a simulation modeling approach that allows the analysis of real-world problems by creating a simulated model that mimics these issues. Through the development of model scenarios, the agent-based simulation model can be examined to assess the impact of decision-making on the entire simulation system. This offers valuable insights into potential outcomes in real systems under similar decision-making scenarios. Unlike deterministic optimization models, agent-based simulation models have the capacity to handle stochastic problems and incorporate uncertainty. Consequently, agent-based simulation models have an advantage over optimization models in representing real system conditions that often involve multiple uncertainties. Moreover, agent-based simulation enables the modeling of interactions among individuals or agents within the environment. This facilitates the observation of spontaneous phenomena, such as agents adapting their mapping paths due to influencing factors, and the subsequent impacts. Furthermore, agent-based simulation helps overcome limitations in terms of time and resources when conducting research on real systems [17].

This study endeavors to develop an agent-based model for assessing post-disaster mapping of Mount Merapi's eruption. The model incorporates a combined route of ground vehicles and drones, considering the impact of depot location and bridge availability on the overall time required for post-disaster mapping assessment. By addressing the previously mentioned problems and proposing

solutions, the study aims to provide insights into the design and evaluation of an effective mapping approach for the aftermath of Mount Merapi's eruption.

## 2. PROPOSED METHOD

### A. Conceptual Model

This study commenced with the development of a conceptual model that offers a comprehensive representation of the post-disaster location mapping process. This conceptual model was subsequently translated into a simulation model. A detailed depiction of the conceptual model illustrating the location mapping process following the eruption of Mount Merapi, which will be the focus of this study, is provided in Fig. 2.

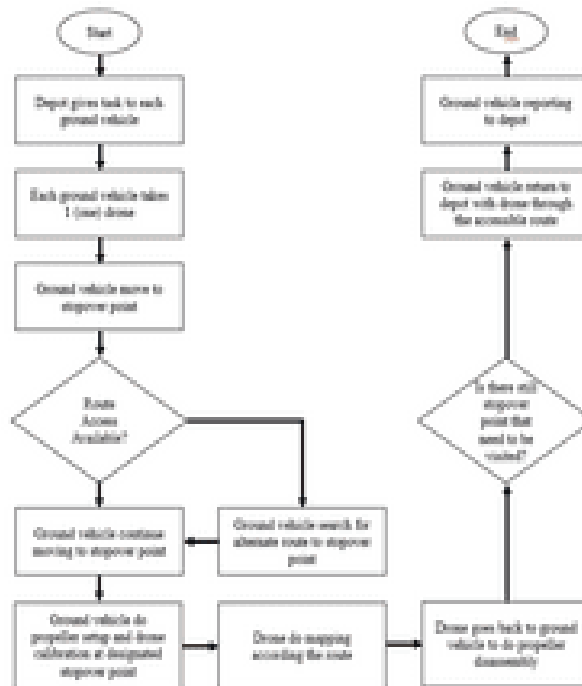


Fig. 2 Conceptual model

### A. Agent-based Simulation Model

This research employed the AnyLogic software to conduct agent-based simulation modeling. The initial step involved data collection on agent behavior, serving as a foundation for establishing the logical rules governing agent behavior, which were subsequently incorporated into the simulation model. The agent-based simulation model encompasses seven distinct types of agents, namely Depots, Stopover Points, Mapping Points, Land Vehicles (Bikes), Drones, Opak Bridges, and Gendol Bridges. The accompanying list provides details on each agent type, including their behavioral rules, quantity, and specific locations.

#### Depot:

1. Depot agents function as both the origin and destination for Ground Vehicles (Bike agents) and Drones.
  2. The Depot agent issues instructions regarding the initiation of the post-disaster location mapping process to the assigned Bike agent.
  3. The Depot agent calculates the overall time required to accomplish a sequence of post-disaster location mapping tasks, starting from the assignment given to each Bike agent until the Bike agent returns with the mapping results report.
- Stopover Point:* The Stopover Point agent assumes a passive role, serving solely as a destination where Bike agents can deploy Drone agents for their operations.

a) *Mapping Point:*

- 1) Mapping Point agents serve as designated locations for Drone agents to map post-disaster areas.
- 2) At the beginning of the simulation, Mapping Point agents are initially in an unmapped state.
- 3) Once a Drone agent initiates mapping at a Mapping Point agent, its status will be updated to "mapped" and it will commence calculating the mapping duration.
- 4) Upon completion of the mapping task by the Drone agent, the Mapping Point agent will update its status to "mapped" and cease the calculation of mapping duration.

b) *Bike:*

- 1) Bike agents utilize motorcycle lanes to travel at a speed ranging from 15 to 30 kilometers per hour.
- 2) The Bike agent is equipped with parameters that determine the sequence of points to visit based on the combined ground vehicle and drone route.
- 3) The Bike agent initiates the post-disaster mapping process once assigned by the Depot agent and begins calculating its duty duration.
- 4) Subsequently, the Bike agent transports a Drone agent to the designated Stopover Point agent.
- 5) In case the Bike agent encounters an Opak Bridge or Gendol Bridge agent during the journey, it promptly assesses the condition of the bridge agent. If the bridge is damaged, the Bike agent adjusts the route to lower ground, following the river until finding an intact bridge agent of the same type. The Bike agent records the successfully crossed Opak Bridge or Gendol Bridge agents to facilitate future crossings.
- 6) Upon reaching the designated Stopover Point agent, the Bike agent signals the start of the mapping process for the carried Drone agent. The Bike agent assumes a passive role and waits until the completion of mapping at the Stopover Point agent, after which the Drone agent is retrieved.
- 7) The Bike agent proceeds to the next destination according to the prescribed route.
- 8) Upon returning to the Depot agent, the Bike agent returns the Drone agent, reports the mapping results to the Depot agent, and concludes its duty duration calculation.

c) *Opak Bridge:* The condition of the Opak Bridge agent can vary, either being intact or damaged, depending on the specific scenario being considered.

d) *Gendol Bridge:* The status of the Gendol Bridge agent can vary, either being functional or damaged, depending on the specific scenario being considered.

Parameter data in this study consisted of 8 (eight) things, namely land vehicle speed data (bike), drone speed data, drone max coverage data, drone battery capacity, drone mapping rate data, propeller setup time data, drone calibration time data, as well as propeller disassembly time data. These data can be seen in Table 1.

Table I. parameter data

Agent	Parameter	Value	Source
Bike	Speed	15 – 30 km/h	[18]
Drone	Speed	16 m/s	[10]
	Battery capacity	30 minutes	[19]
	Max coverage	151668 m <sup>2</sup>	Pix4DCapture
	Mapping rate	0,00011209 minutes/m <sup>2</sup>	
	Propeller setup time	triangular(14.,25.6,18.2) seconds	[20]
	Drone calibration time	triangular(34.,46.3,42.6) seconds	
Propeller disassembly time	triangular(14.,21.1,14.) seconds		

B. *Verification and Validation*

To ensure the suitability of the developed simulation model in accurately representing real-world scenarios, it is crucial to conduct feasibility tests. Verification and validation tests are common approaches used to assess the feasibility of simulation models. Verification involves comparing the

simulation model to the underlying conceptual model to ensure its compatibility. Successful verification indicates that the model runs smoothly without any programming errors when executed based on the conceptual model. AnyLogic software offers the option to perform verification tests by utilizing features like "Build Model" or constructing the simulation model. These features provide valuable insights into the presence or absence of errors in the implemented programming algorithms.

Once the verification test has been conducted, the subsequent step involves performing a validation test on the simulation model. Validation aims to assess whether the simulation model effectively captures the dynamics of the real system it represents. One technique commonly employed for validating a simulation model against a real system is known as Face Validation. This technique involves demonstrating that the simulation model's characteristics and operational mechanisms exhibit similarities to those observed in the real-world system being modeled [21]. In the case of AnyLogic software, this can be accomplished by executing the developed simulation model and comparing its performance with the actual system to evaluate its appropriateness.

*C. Developing Simulation Scenarios*

Two parameters serve as the foundation for scenario development in this study: the depot parameter and the damage level parameter of bridge facilities, which are determined based on the KRB (Kawasan Rawan Bencana). The simulation will consider the following conditions for scenario development:

1. The first condition involves intact bridge facilities, which will be applied to the nine designated depots.
2. The second condition involves damaged bridge facilities in the KRB III area. This condition will be applied to the nine designated depots.
3. The third condition involves damaged bridge facilities in both the KRB III and KRB II areas. This condition will also be applied to the nine designated depots.

To assess the impact of different levels of damage to bridge facilities on each depot location, each condition of damage will be applied to each depot. This approach allows for the examination of the specific effects of each damage level on individual depots. Consequently, a total of 27 scenarios will be conducted in this study, derived from the three damage conditions applied to the nine depots. The complete list of scenarios employed in this research can be found in Table 2.

Table II. Scenarios Development List

Scenario	Parameter		Scenario	Parameter	
	Depot	Damage Level		Depot	Damage Level
1	Depot 1	Normal	15	Depot 5	KRB II & KRB III
2	Depot 1	KRB III	16	Depot 6	Normal
3	Depot 1	KRB II & KRB III	17	Depot 6	KRB III
4	Depot 2	Normal	18	Depot 6	KRB II & KRB III
5	Depot 2	KRB III	19	Depot 7	Normal
6	Depot 2	KRB II & KRB III	20	Depot 7	KRB III
7	Depot 3	Normal	21	Depot 7	KRB II & KRB III
8	Depot 3	KRB III	22	Depot 8	Normal
9	Depot 3	KRB II & KRB III	23	Depot 8	KRB III
10	Depot 4	Normal	24	Depot 8	KRB II & KRB III
11	Depot 4	KRB III	25	Depot 9	Normal
12	Depot 4	KRB II & KRB III	26	Depot 9	KRB III
13	Depot 5	Normal	27	Depot 9	KRB II & KRB III
14	Depot 5	KRB III	-	-	-

### 3. RESULTS AND DISCUSSIONS

The AnyLogic software was used to create the agent-based model, which consists of several graphical editor windows. These windows include the main graphical editor, as well as separate graphical editors for each agent, and an experiment graphical editor. The sequence of graphical editors, namely the main graphical editor, Depot agent graphical editor, Stopover Point agent graphical editor, Mapping Point agent graphical editor, Bike agent graphical editor, Drone agent graphical editor, Opak Bridge agent graphical editor, Gendol Bridge agent graphical editor, and experiment graphical editor, can be observed in Figures 3 to 11, respectively.

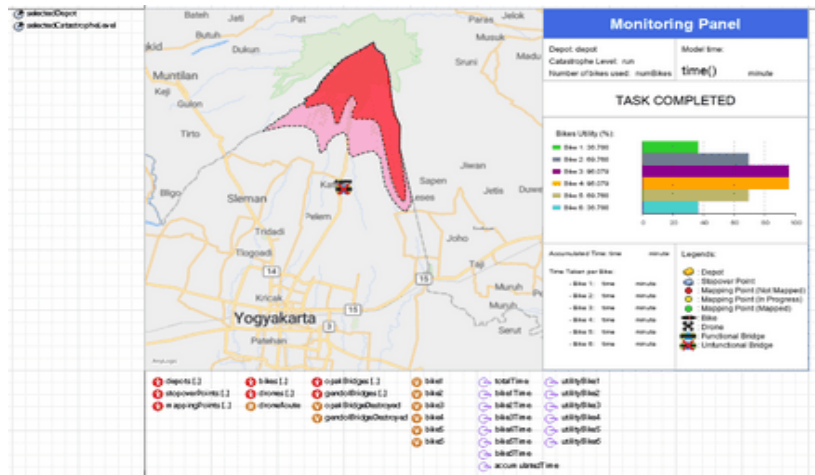


Fig. 3 Main graphical editor

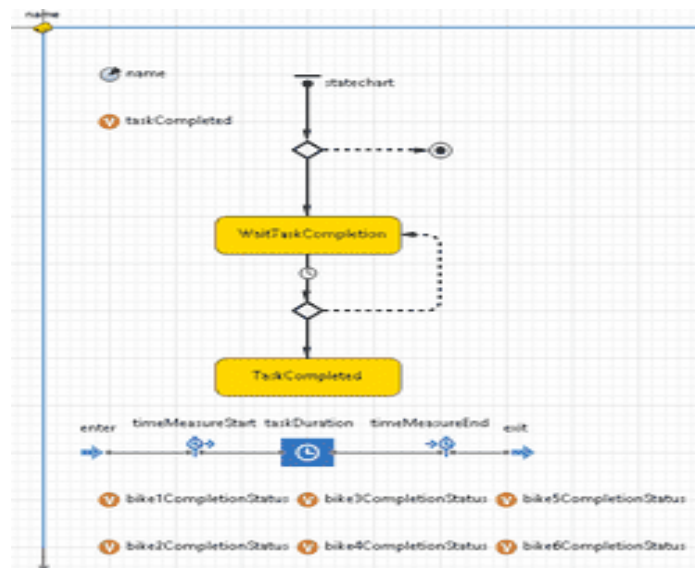


Fig. 4 Depot agent graphical editor

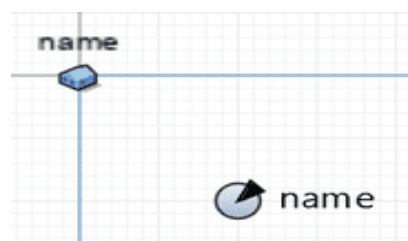


Fig. 5 Stopover Point agent graphical editor

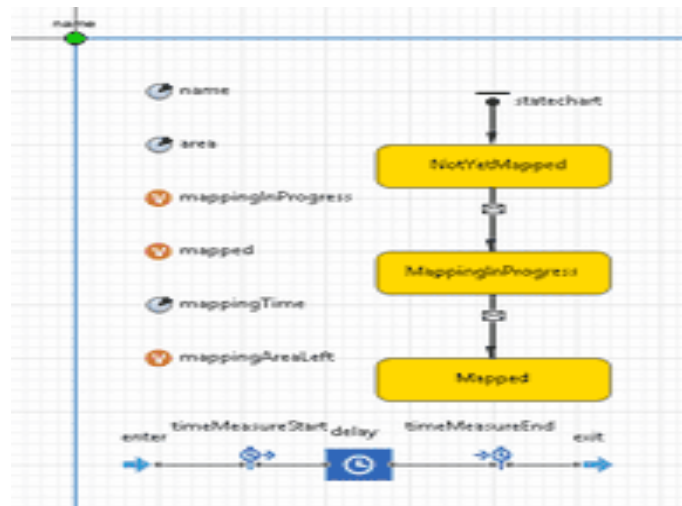


Fig. 6 Mapping Point agent graphical editor

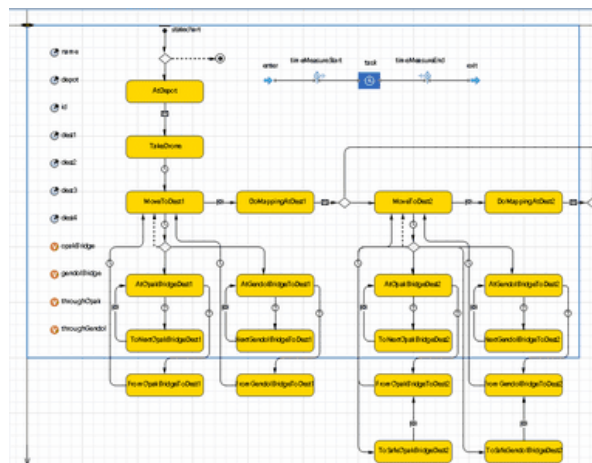


Fig. 7 Bike agent graphical editor

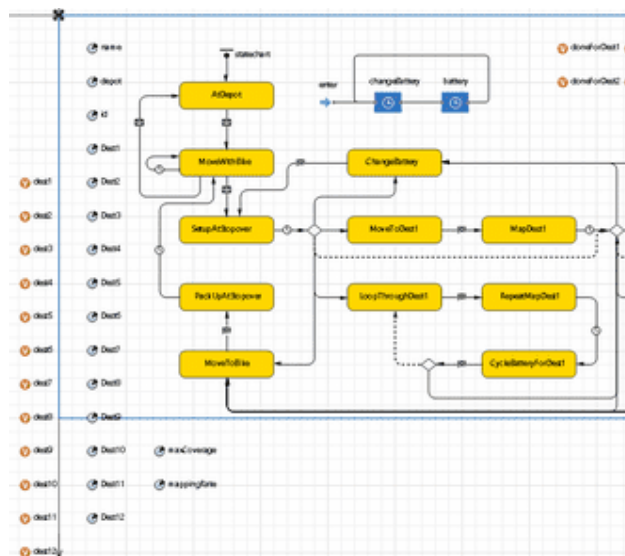


Fig. 8 Drone agent graphical editor

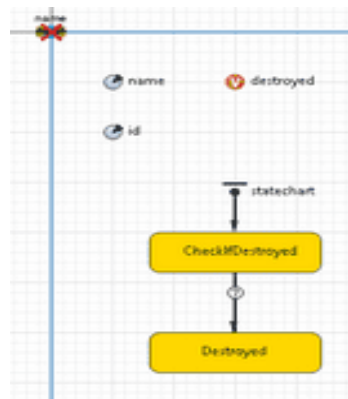


Fig. 9 Opak Bridge agent graphical editor

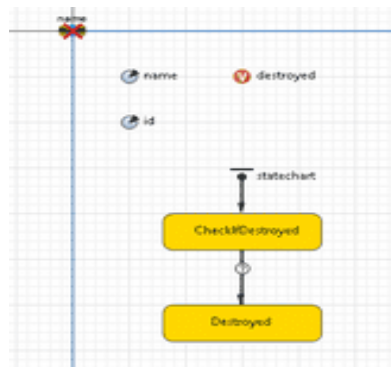


Fig. 10 Gendol Bridge agent graphical editor

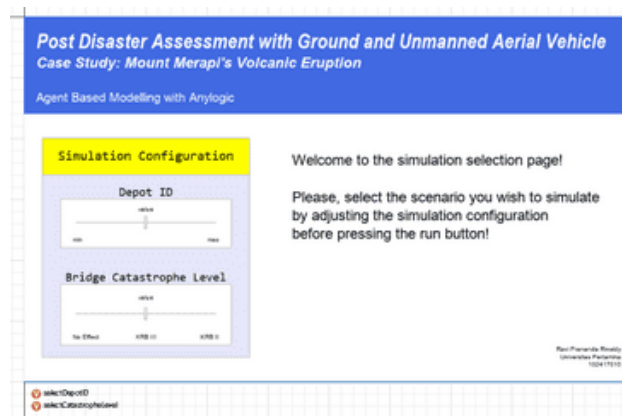


Fig. 11 Experiment graphical editor

Once all graphical editors have been finalized, the subsequent stage involves building the model to identify any potential errors. In this research, no error markers were detected upon completing the model building process for the developed simulation model. As a result, it can be concluded that the simulation model has successfully undergone the verification test.

Upon conducting the face validation technique for model validation, it was observed that the simulation model accurately reflects the mechanisms and properties that would occur in a real-world scenario. This indicates that the simulation model has successfully passed the validation test utilizing the face validation technique.

In this study, the agent-based simulation employed a stochastic model, which contributes to the uniqueness of results in each run. Replication serves as a technique to enhance the representativeness and accuracy of the simulation outcomes based on the utilized model [20]. Consequently, the minimum number of replications needed for each scenario was initially established. The

determination of the required replications was performed using 30 sample data points, employing the "accumulatedTime" data from the model as a comparative parameter, and applying a confidence level of 95%. The variables utilized in the determination of the replication count are presented in Table 3.

Table I. Calculation Variables For Determining The Number Of Replications

Variable	Value
Confidence Level	95%
Significance Level	0.05
Sample Size(n)	30
n-1	29
$\alpha / 2$	0.025
t(29), 0.025	2.045
z(0.025)	1.96

The calculation performed in this study determined that each scenario required a minimum of 28 replications, which remained consistent across all scenarios. As the sample size utilized for determining the replication count was 30, the data obtained can be deemed representative and will be utilized in the subsequent analysis of the study's findings.

A. Comparison with Optimization Model

In this study, an agent-based simulation model was developed to map the post-disaster eruption locations of Mount Merapi in DI Yogyakarta. The model incorporates a combination route involving land vehicles and drones. The simulation model is based on an optimization model that addresses similar cases, with the objective of minimizing the overall processing time [10]. A comparison of the total processing time per depot between the agent-based simulation model and the referenced optimization models is presented in Table 4 and Fig. 12.

According to the data presented in Table 4 and Fig. 12, there is a notable disparity in the total processing time between the optimization model and the simulation model, with a range of deviation between 68% and 81%, and an average deviation of 73%. The simulation model demonstrates a longer total processing time compared to the optimization model, as it takes into account various uncertain variables that influence the system. These variables include propeller setup time, drone calibration time, propeller disassembly time, as well as parameter adjustments based on real system conditions, such as battery capacity and land vehicle speed during the post-disaster location mapping process.

Table IV. Comparison Of Total Processing Time Per Depot Between Optimization Models And Simulation Models

Depot	Total Processing Time (Minute)		Deviation
	Optimization	Simulation	
Depot 1	644.809	1164.841	81%
Depot 2	611.519	1080.818	77%
Depot 3	586.239	1007.562	72%
Depot 4	615.989	1066.960	73%
Depot 5	639.349	1123.546	76%
Depot 6	683.899	1202.430	76%
Depot 7	573.039	966.824	69%

Depot	Total Processing Time (Minute)		Deviation
	Optimization	Simulation	
Depot 8	609.229	1030.260	69%
Depot 9	601.159	1012.852	68%
Average			73%

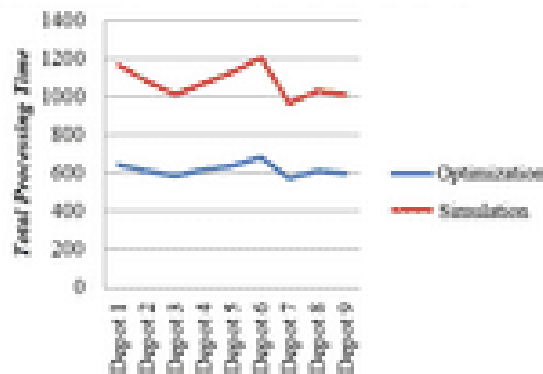


Fig. 12 Comparison of total processing time per depot between optimization models and simulation models

D. The Impact of Bridge Facility Damage Level on Total Processing Time Value

In this research, various scenarios were created to examine the impact of different levels of damage to bridge facilities on the total processing time per depot. The scenarios considered three conditions of damage: normal, KRB III, and KRB II & KRB III. These damage level conditions were then applied to the 9 depot locations, resulting in a total of 27 scenarios. The relationship between the level of damage to bridge facilities and the corresponding total processing time per depot can be observed in Table 5 and Fig. 13.

Table II. Impact Of Damage Level Of Bridge Facilities On Total Processing Time Per Depot

Depot	Total Processing Time Based on Damage Level (Minute)			Deviation to Normal Condition	
	Normal	KRB III	KRB II & KRB III	KRB III	KRB II & KRB III
Depot 1	1164.841	1246.131	1421.518	7%	22%
Depot 2	1080.818	1100.147	1384.240	2%	28%
Depot 3	1007.562	1029.453	1348.847	2%	34%
Depot 4	1066.960	1200.508	1505.500	13%	41%
Depot 5	1123.546	1120.750	1120.745	0%	0%
Depot 6	1202.430	1198.852	1480.112	0%	23%
Depot 7	966.824	1073.010	1081.844	11%	12%
Depot 8	1030.260	1171.134	1190.204	14%	16%
Depot 9	1012.852	1188.199	1179.154	17%	16%
Average				7%	21%

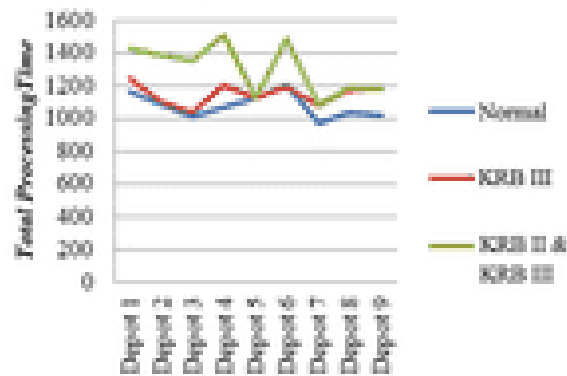


Fig. 13 Impact of Damage Level of Bridge Facilities on Total Processing Time per Depot

Based on the data presented in Table 5 and Fig. 13, it is evident that the level of damage to the bridge facilities significantly affects the total processing time per depot. On average, there is a deviation of 7% for KRB III and 21% for KRB II & KRB III. However, an interesting observation can be made from the analysis of Table 5 and Fig. 13. One particular depot, Depot 5, appears to be unaffected by the level of damage to the bridge facilities. This is due to the strategic location of Depot 5, which is situated at a lower elevation than the bridge facilities in KRB II & KRB III (Fig. 14). Consequently, the route used by Depot 5 does not involve crossing the Gendol River or the Opak River.

Moreover, certain depots such as Depot 2, Depot 3, and Depot 6 experienced a noticeable increase in total processing time exceeding 5% when the level of facility damage was elevated to KRB II & KRB III. Conversely, Depot 7, Depot 8, and Depot 9 exhibited an opposite trend to Depot 2, Depot 3, and Depot 6. When the level of damage to the bridge facilities was increased to KRB III, these three depots experienced an increase in total processing time exceeding 5%. However, when the damage was further escalated from KRB III to KRB II & KRB III, these three depots did not display a significant increase in total processing time surpassing 5%, as evident from the difference in total processing time between the KRB III and KRB II & KRB III levels of damage to the bridge facilities.

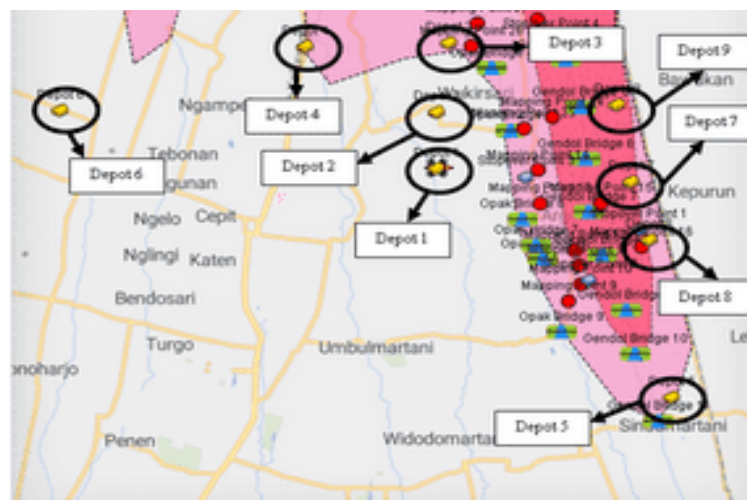


Fig. 14 Visualization of Depot Locations on AnyLogic Software

Based on the analysis of the deviations in the total processing time per depot due to the level of damage to the bridge facilities in KRB III and KRB II & KRB III (Table 5 and Fig. 13), as well as the visualization of depot locations in AnyLogic software (Fig. 14), it can be observed that depots situated east of Kali Gendol, namely Depot 7, Depot 8, and Depot 9, are more susceptible to the impact of the level of damage to the bridge facilities in KRB III compared to the impact of the level of damage to the bridge facilities in KRB II. Conversely, depots located west of the Opak River exhibit a greater

sensitivity to the impact of the level of damage to the bridge facilities in KRB II compared to the impact of the level of damage to the bridge facilities in KRB III.

Based on the analysis of Table 5, Fig. 13, and Fig. 14, valuable information can be derived regarding the depot with the most optimal location and route among the other depots, indicated by the smallest total processing time for each level of damage to the bridge facilities. Depot 7 emerges as the most appropriate choice when there is no damage to the bridge facilities or when the damage level reaches KRB II and KRB III, with total processing time values of 966.824 and 1081.844 minutes, respectively. On the other hand, if the damage level only extends to KRB III, Depot 3 is deemed the most suitable depot, with a total processing time value of 1029.453 minutes.

*E. The Impact of Bridge Facility Damage Level on Total Completion Time Value*

In post-disaster logistics, the prompt completion of tasks is of utmost importance. Therefore, the time required for the disaster mapping process serves as a crucial factor to consider. Previously, an analysis was conducted using the total processing time indicator, which represents the cumulative time for each task within a system. This indicator effectively measures the overall work time required for completing various tasks. However, when applied to post-disaster logistics, particularly in the case of location mapping, these indicators may not accurately reflect the real-world scenario. This discrepancy arises because the total processing time assumes sequential execution of tasks without breaks or concurrent work. To address these limitations, an alternative approach is to utilize the total completion time indicator [22].

The total completion time encompasses both the duration of a task and its placement within the scheduling timeframe. This indicator provides an accurate representation of the actual time required to complete the entire task, considering the task scheduling in real-world conditions [22]. In the context of this study's agent-based simulation for post-disaster location mapping, the total completion time indicator is well-suited. This is because the model incorporates six bike agents that perform their tasks concurrently, allowing the indicator to effectively demonstrate the actual time needed for the complete post-disaster location mapping process. The comparison of the impact of bridge facility damage levels on the total completion time per depot is presented in Table 6 and Figure 15.

Table III. Impact of Damage Level of Bridge Facilities on Total Completion Time per Depot

Depot	Total Completion Time Based on Damage Level (Minute)			Deviation to Normal Condition	
	Normal	KRB III	KRB II & KRB III	KRB III	KRB II & KRB III
Depot 1	243.159	316.536	317.279	30%	30%
Depot 2	248.410	249.763	285.217	1%	15%
Depot 3	268.267	267.736	343.612	0%	28%
Depot 4	237.727	280.650	349.975	18%	47%
Depot 5	290.464	290.979	291.838	0%	0%
Depot 6	282.482	292.878	376.014	4%	33%
Depot 7	250.910	280.525	282.439	12%	13%
Depot 8	205.259	241.265	244.763	18%	19%
Depot 9	233.999	273.833	268.591	17%	15%
Average				11%	22%

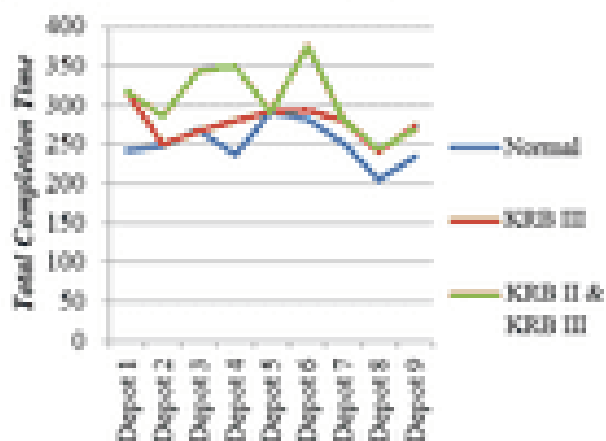


Fig. 15 Impact of damage level of bridge facilities on total completion time per depot

Based on the findings presented in Table 6 and Fig. 15, it can be observed that the level of damage to the bridge facilities significantly affects the total completion time per depot, with an average deviation of 11% for KRB III and 22% for KRB II & KRB III. The impact of the damage level on the total completion time per depot (Table 6 and Fig. 15) mirrors the impact observed on the total processing time per depot (Table 4 and Fig. 13), except for Depot 1. Interestingly, even though Depot 1 is situated east of the Opak River, it is more influenced by the damage to the bridge facilities in KRB III compared to KRB II. This discrepancy arises because although Depot 1 is located on the east side of the Opak River, it still requires a land vehicle route through Kali Gendol. Consequently, the land vehicles passing through Kali Gendol must opt for an alternative route that is longer than the initial path, resulting in increased travel time. As the total completion time is determined by the completion time of the land vehicle with the longest duration, any increase in travel time for a single land vehicle can significantly impact the overall total completion time value.

Other Based on the analysis of Table 6, Fig. 15, and Fig. 14, it is possible to identify the depot with the optimal location and route among the other depots based on the smallest total completion time value for each level of damage to the bridge facilities. Depot 8 emerges as the most suitable depot for various scenarios, including situations without any damage to the bridge facilities, cases where the damage reaches KRB III, and instances where the damage extends to both KRB II and KRB III. The total completion time values for Depot 8 are recorded as 205,259 minutes when no damage occurs, 241,265 minutes when the damage level reaches KRB III, and 244,763 minutes when the damage level encompasses both KRB II and KRB III bridge facilities.

*F. The Impact of Bridge Facility Damage Level on the Average Utilities of Land Vehicles and Drones per Depot*

In this research, relevant data was gathered concerning the average utility of land vehicles and drones per depot. This data was obtained from simulations conducted to investigate the potential relationship between the level of damage to bridge facilities and the average utility value of land vehicles and drones. The effects of the level of damage to bridge facilities on the average utility of land vehicles and drones per depot are presented in Table 7 and Fig. 16.

**Table IV. Impact of Damage Level of Bridge Facilities on the Average Utilities of Land Vehicles and Drones per Depot**

Depot	Average Utility of Land Vehicles and Drones			Deviation to Normal Condition	
	Normal	KRB III	KRB II & KRB III	KRB III	KRB II & KRB III
Depot 1	80%	66%	75%	17%	6%
Depot 2	73%	73%	81%	1%	12%
Depot 3	63%	64%	66%	2%	5%
Depot 4	75%	72%	72%	4%	4%

Depot	Average Utility of Land Vehicles and Drones			Deviation to Normal Condition	
	Normal	KRB III	KRB II & KRB III	KRB III	KRB II & KRB III
Depot 5	65%	64%	64%	0%	1%
Depot 6	71%	69%	66%	4%	7%
Depot 7	64%	64%	64%	1%	1%
Depot 8	84%	81%	81%	3%	3%
Depot 9	72%	73%	73%	0%	2%
<b>Rata-Rata</b>				4%	4%

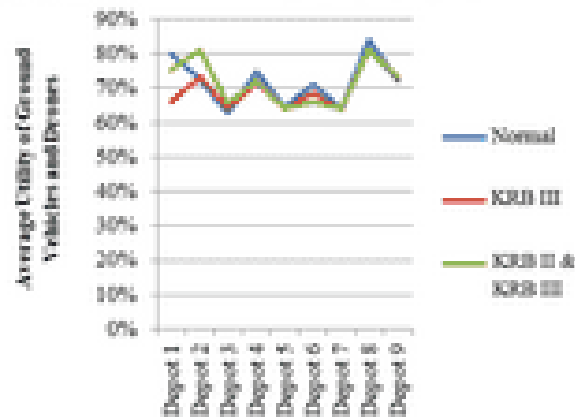


Fig. 16 Impact of Damage Level of Bridge Facilities on the Average Utilities of Land Vehicles and Drones per Depot

According to the data presented in Table 7 and Fig. 16, there is no substantial correlation observed between the level of damage to bridge facilities and the average utility of land vehicles. This is evident from the average deviation, which remains below 5% as indicated in Table 7 and Fig. 16, with an average deviation value of 4% for both levels of bridge facility damage.

### G. Practical Implications

Through this research, valuable insights into the potential impacts on real-world systems due to facility damage and subsequent road closures during the post-disaster location mapping process have been obtained. Stakeholders should carefully consider the selection of depot locations for conducting this mapping process. Merely choosing depots in close proximity to disaster-affected areas does not guarantee expedited completion of the post-disaster mapping process. Instead, depot locations must ensure adequate road access for land vehicles and be resilient to damage caused by disasters. Moreover, they should have alternative access routes that are equally robust and resilient. This ensures that in the event of road closures on primary routes, land vehicles can effortlessly switch to alternative routes that are equally reliable and efficient.

This research has also provided valuable information regarding the role of land vehicle agents' adaptability in responding to unexpected road closures, which can significantly affect the overall completion time of the post-disaster mapping process. Consequently, stakeholders should carefully evaluate and incorporate alternative routes into their planning to mitigate the potential impact of unforeseen circumstances in the field. Furthermore, considering the adoption of more sustainable routes is advisable to minimize the risk of inaccessible roads for land vehicles during post-disaster mapping assessments.

#### 4. CONCLUSIONS

This research focuses on the design of an agent-based simulation model for the post-disaster location mapping process, which integrates land vehicles and drones while considering the availability of access roads and depot locations. Various scenarios have been developed by incorporating depot location parameters and the damaged condition of bridge facilities based on the KRB. A total of 27 scenarios were simulated to analyze the impact of bridge facility damage on different depot locations. The findings indicate that depots situated east of the Opak River are more susceptible to the effects of bridge facility damage at KRB II, while depots located west of Kali Gendol are more influenced by damage at KRB III. Consequently, such impacts can lead to an increase in both total processing time and total completion time. This can be attributed to the interactions between land vehicles and bridge facilities, as the land vehicles autonomously seek alternative routes when encountering damaged bridges, resulting in extended distances and travel durations.

In addition to the analysis of agent behavior and its implications, this study also identifies the optimal depot location among nine candidate locations, taking into account the specific bridge facility damage scenarios and relevant time indicators. The agent-based simulation model reveals that in scenarios without any bridge facility damage or with damage at KRB II and III, Depot 7 emerges as the most favorable location based on the total processing time indicator, with respective times of 966,824 and 1,081,844 minutes. This finding aligns with the optimization model used as a reference in this study, where Depot 7 was selected as the best location based on the total processing time indicator for undamaged bridge facilities, with a time of 573,039 minutes. In the case of damage at KRB III, the simulation model suggests that Depot 3 exhibits the optimal location based on the total processing time indicator, with a time of 1,029,453 minutes. Moreover, when considering the total completion time indicator, Depot 8 is identified as the depot location with the shortest overall completion time, regardless of the presence of bridge facility damage. Specifically, it demonstrates the shortest completion time in scenarios with undamaged bridge facilities (205,259 minutes), damage at KRB III (241,265 minutes), and damage at both KRB II and KRB III (244,763 minutes).

#### REFERENCES

- [1] A. S. Masten and F. Motti-Stefanidi, "Multisystem Resilience for Children and Youth in Disaster: Reflections in the Context of COVID-19," 2020.
- [2] M. Aleksandranova, S. Balasko, M. Kaltenborn, D. Malerba, P. Mucke, O. Neuschafer, K. Radtke, R. Prutz, C. Strupat, D. Weller and N. Wiebe, "WorldRiskReport 2021," Bundnis Entwicklung Hilft, 2021.
- [3] N. A. Pambudi, "Geothermal power generation in Indonesia, a country within the ring of fire: Current status, future development and policy," *Renewable and Sustainable Energy Reviews*, 2017.
- [4] J. Zschau, R. Sukhyar, M. A. Purbawinata, B.-G. Luhr and M. Westerhaus, "The Merapi Project - Interdisciplinary Monitoring of a High-Risk Volcano as a Basis for an Early Warning System," *Early Warning Systems for Natural Disaster Reduction*, pp. 527-532, 2003.
- [5] E. Hariyono and S. Liliyasi, "The characteristic of volcanic eruption in Indonesia," *Volcanoes: Geological and Geophysical Setting, Theoretical Aspect and Numerical Modelling, Applications to Industry and Their Impact on The Human Health*, p. 73, 2018.
- [6] PVMBG, "G. Merapi: Pusat Vulkanologi dan Mitigasi Bencana Geologi," Pusat Vulkanologi dan Mitigasi Bencana Geologi, 3 June 2014. [Online]. Available: <https://vsi.esdm.go.id/index.php/gunungapi/data-dasar-gunungapi/542-g-merapi?start=1>.
- [7] R. Gertisser, S. J. Charbonnier, J. Keller and X. Quidelleur, "The geological evolution of Merapi

- volcano, Central Java, Indonesia," *Bulletin of Volcanology*, pp. 1213-1233, 2012.
- [8] I. H. Sawalha, "A contemporary perspective on the disaster management cycle," 2020.
- [9] S. M. H. Boroujeni, "Post Disaster Needs Assessment (PDNA)," *Journal of Disaster & Emergency Research*, pp. 124-125, 2019.
- [10] A. A. N. P. Redi, Sopha, B. Maya, A. M. S. Asih and R. I. Liperda, "Collaborative Hybrid Aerial and Ground Vehicle Routing for Post-Disaster Assessment," *Sustainability*, vol. 13, no. 22, p. 12841, 2021.
- [11] R. I. Liperda, A. A. N. P. Redi, N. S. Sekaringtyas, H. B. Astiana, B. M. Sopha and A. M. S. Asih, "Simulated Annealing Algorithm Performance on Two-Echelon Vehicle Routing Problem-Mapping Operation with Drones," in *2020 IEEE International Conference on Industrial Engineering and Engineering Management*, Singapore, 2020.
- [12] B. E. Oruc and B. Y. Kara, "Post-disaster assessment routing problem," *Transportation Research Part B: Methodological*, vol. 116, pp. 76-102, 2018.
- [13] M. Aljehani and M. Inoue, "Performance Evaluation of Multi-UAV System in Post-Disaster Application: Validated by HITL Simulator," *IEEE Access*, pp. 64386-64400, 2019.
- [14] N. Sasmita, "The Eruption of Mount Kelud in 1919: It's Impact and Mitigation Efforts," in *1st International Conference on Social Sciences and Interdisciplinary Studies (ICSSIS 2018)*, 2019.
- [15] M. M. Sari, "Aplikasi peta Kawasan Rawan Bencana (KRB) dalam analisa sebaran korban erupsi GA. Merapi 2010," *Jurnal Spasial*, pp. 10-20, 2019.
- [16] D. Muravev, H. Hu, A. Rakhmangulov and P. Mishkurov, "Multi-agent optimization of the intermodal terminal main parameters by using AnyLogic simulation platform: Case study on the Ningbo-Zhoushan Port," *International Journal of Information Management*, 2020.
- [17] M. Dmitri, h. Hu, A. Rakhmangulov and P. Mishkurov, "Multi-agent optimization of the intermodal terminal main parameters by using AnyLogic simulation platform: Case study on the Ningbo-Zhoushan Port," *International Journal of Information Management*, 2020.
- [18] E. Bonabeau, "Agent-based modeling: Methods and techniques for simulating human systems," *Proceedings of the National Academy of Sciences*, pp. 7280-7287, 2002.
- [19] E. Bonabeau, "Agent-based modeling: Methods and techniques for simulating human systems," *Proceedings of the National Academy of Sciences*, pp. 7280-7287, 2002.
- [20] Volcanic Ashfall Impacts Working Group, "Roads & Highway: Transportation: Impacts & Mitigation: Volcanic Ashfall Impacts Working Group," Volcanic Ashfall Impacts Working Group, 12 November 2022. [Online]. Available: [https://volcanoes.usgs.gov/volcanic\\_ash/roads\\_highways.html](https://volcanoes.usgs.gov/volcanic_ash/roads_highways.html).
- [21] DJI, "Phantom 4 Pro V2.0: DJI," DJI, January 2020. [Online]. Available: <https://www.dji.com/id/phantom-4-pro-v2>.
- [22] R. Fridayanti, "Perancangan Model Simulasi Diskrit untuk Rute Pemetaan Area Terdampak Bencana Menggunakan Kombinasi Kendaraan Darat dan Drone," Universitas Pertamina,

Jakarta, 2022.

- [23] U. Wilensky and W. Rand, *An Introduction to Agent-Based Modeling*, London: The MIT Press, 2015.
- [24] C. Low and W.-Y. Lin, "Minimizing the total completion time in a single-machine scheduling problem with a learning effect," *Applied Mathematical Modelling*, pp. 1946-1951, 2011.